Oligomeric Interactions between Phospholamban Molecules Regulate Ca-ATPase Activity in Functionally Reconstituted Membranes†

Qing Yao, Linda T. L. Chen, Jinhui Li, Kimberley Brungardt, Thomas C. Squier, and Diana J. Bigelow*

Biochemistry and Biophysics Section, Department of Molecular Biosciences, University of Kansas, Lawrence, Kansas 66045-2106

Received December 20, 2000; Revised Manuscript Received March 27, 2001

ABSTRACT: Phospholamban (PLB) is a major target of the β-adrenergic cascade in the heart, and functions as an endogenous inhibitor of Ca-ATPase transport activity. To identify whether oligomeric interactions between PLB molecules are involved in regulating Ca-ATPase transport activity, we have investigated functional interactions between PLB and the Ca-ATPase in proteoliposomes of purified PLB functionally co-reconstituted with the SERCA2a isoform of the Ca-ATPase isolated from cardiac sarcoplasmic reticulum (SR). The calcium sensitivity of this reconstituted preparation and functional stimulation by cAMP-dependent protein kinase (PKA) are virtually identical to those of the Ca-ATPase in cardiac SR microsomes, ensuring the functional relevance of this reconstituted preparation. Interactions between PLB molecules were measured following covalent modification of the single lysine (i.e., Lys^3) in PLB isolated from cardiac SR membranes with fluorescein isothiocyanate (FITC) prior to co-reconstitution with the Ca-ATPase. FITC modification of PLB does not interfere with the ability of PLB to inhibit the Ca-ATPase, since FITC-PLB co-reconstituted with the Ca-ATPase exhibits a similar calcium dependence of Ca-ATPase activation to that observed in native SR membranes. Thus, the functional arrangement of PLB with the Ca-ATPase is not modified by FITC modification. Using changes in the anisotropy of FITC-PLB resulting from fluorescence resonance energy transfer (FRET) between proximal PLB molecules to measure the average size and spatial arrangement of FITC chromophores, we find that PLB self-associates to form oligomers whose spatial arrangement with respect to one another is in agreement with earlier suggestions that PLB exists predominantly as a homopentamer. The inability of PKA to activate PLB following covalent modification with FITC permits functional interactions between PLB molecules associated with the Ca-ATPase activation to be identified. A second-order loss of Ca-ATPase activation by PKA is observed as a function of the fractional contribution of FITC-PLB, indicating that PKA-dependent activation of two PLB molecules within a quaternary complex containing the Ca-ATPase is necessary for activation of the Ca-ATPase. We suggest that the requirement for activation of two PLB molecules by PKA represents a physiological mechanism to ensure that activation of the Ca-ATPase following β-adrenergic stimulation in the heart only occurs above a threshold level of PKA activation.

The 52 amino acid membrane protein phospholamban (PLB)[1] regulates the sarcoplasmic reticulum (SR) Ca-ATPase in response to β-adrenergic stimulation of the heart (*1, 2*). Phosphorylation of PLB induced by either cAMP-dependent kinase (PKA) or calmodulin-dependent kinase at Ser_{16} or Thr_{17}, respectively, results in an altered interaction with the Ca-ATPase that facilitates rate-limiting structural transitions of this active transport protein (*3*). Amino acid residues within the cytoplasmic domains of both the Ca-ATPase ($DKKDPV_{401}$) and PLB (Glu_2 to Ile_{18}) have been identified that provide essential conformational features for these interactions as evidenced by the loss of the PLB-dependent shift in calcium activation of the Ca-ATPase when these residues are individually mutated (*4, 5*). Interactions between transmembrane domains of PLB and the ATPase have also been implicated (*6*), suggesting that the presence of the phosphoryl group on PLB induces long-range structural effects within PLB that may directly modify the calcium sensitivity of the Ca-ATPase.

Information regarding the secondary structure of PLB has been obtained from circular dichroism (CD) and NMR measurements of PLB in organic solvents and detergent micelles, as well as Fourier transform infrared (FT-IR) and CD measurements of PLB reconstituted into lipid bilayers (*7*−*12*). The results of these studies are consistent with predictions of PLB secondary structure based on its sequence and have further suggested possible tertiary and quaternary structures (*11, 13*−*15*). Early studies have interpreted the

† Supported by National Institutes of Health Grants AG12275 and GM46837 and the American Heart Association (Kansas affiliate).

* Correspondence should be addressed to this author. Tel: (785)-864-3831; FAX: (785)-864-5321; E-mail: dbigelow@falcon.cc.ukans.edu.

[1] Abbreviations: ATP, adenosine 5′-triphosphate; BSA, bovine serum albumin; BAPTA, 1,2-bis(2-aminophenoxy)ethane-*N*,*N*,*N*′,*N*′-tetraacetic acid; Ca-ATPase, Ca^{2+}- and Mg^{2+}-dependent calcium pump; cAMP, adenosine 3′,5′-cyclic monophosphate; DTT, dithiothreitol; EGTA, ethylene glycol bis(β-aminoethyl ether)-*N*,*N*,*N*′,*N*′-tetraacetic acid; FITC, fluorescein 5-isothiocyanate; MOPS, 3-(*N*-morpholino)propanesulfonic acid; PKA, cAMP-dependent protein kinase; PLB, phospholamban; PMSF, phenylmethylsulfonyl fluoride; SR, sarcoplasmic reticulum.

10.1021/bi002891t CCC: $20.00
Published on Web 05/03/2001

high propensity of PLB for aggregation in aqueous solution and its heat-labile association as higher molecular weight species (predominantly pentamers) in both SDS and $C_{12}E_8$ detergent micelles as evidence that PLB also exists as an oligomer in the native SR membrane (*16*). Consistent with this interpretation, recent spin-label EPR and fluorescence resonance energy transfer (FRET) experiments have provided direct physical evidence for the self-association of PLB as stable oligomers in lipid bilayers (*17*−*19*). However, the oligomeric state of PLB responsible for regulation of Ca-ATPase activity remains unclear. It has been suggested that the inhibitory species of PLB is a monomer, since (i) mutants of PLB that stabilize the monomeric state are more effective inhibitors of the Ca-ATPase and (ii) direct physical measurements indicate that the average oligomeric size of PLB is decreased in the presence of the Ca-ATPase (*19*−*23*). However, full activation of the Ca-ATPase requires the phosphorylation of multiple PLB molecules (*24*, *25*), suggesting that oligomeric interactions between PLB molecules may be important in the activation of the Ca-ATPase. To address the functional oligomeric state of PLB in association with the Ca-ATPase, we have used spectroscopic and functional measurements of the interactions between PLB and the cardiac SR Ca-ATPase (SERCA2a) within reconstituted and fully functional proteoliposomes. These measurements suggest that the phosphorylation of two PLB molecules by cAMP-dependent protein kinase (PKA) is necessary for the observed activation of the Ca-ATPase, consistent with earlier suggestions that the functional species of PLB is a dimer (*26*). Therefore, the activation of multiple PLB molecules may represent an important regulatory mechanism to ensure the coordinated activation of the Ca-ATPase following β-adrenergic stimulation, also facilitating rapid inactivation of the Ca-ATPase by phosphatases.

EXPERIMENTAL PROCEDURES

Materials. $CaCl_2$ standard solutions were purchased from VWR (St. Louis, MO). MOPS, KCl, and ultracentrifugation grade sucrose were purchased from Fisher (Fair Lawn, NJ). Reactive Red 120 and the detergent *N*-octyl-β-D-glucopyranoside were obtained from ICN (Aurora, OH). The detergent polyoxyethylene 8 lauryl ether ($C_{12}E_8$) was purchased from Nikko Chemical Co. (Hokkaido, Japan). Sepharose CL-4B, ADP, PKA, cAMP, ATP, $MgCl_2$, the calcium ionophore A23187, the potassium ionophore valinomycin, EGTA, and fluorescein isothiocyanate (FITC) were purchased from Sigma (St. Louis, MO). The protonophore CCCP (carbonyl cyanide 3-chlorophenylhydrazone) was purchased from Fluka (Buchs, Switzerland). Egg phosphatidylcholine, egg phosphatidylethanolamine, egg phosphatidic acid, brain phosphatidylserine, egg sphingomyelin, and soybean phosphatidylinositol were obtained from Avanti Polar Lipids (Alabaster, AL). Primary antibodies against the SERCA2a (cardiac) isoform of the Ca-ATPase and against PLB were obtained from Affinity Bioreagents (Golden, CO) and Upstate Biotechnology (Lake Placid, NY). Peroxidase-linked goat anti-rabbit antibody was from Zymed (South San Francisco, CA). Calcium Green-5N was obtained from Molecular Probes (Corvallis, OR). The monoclonal antibody directed against PLB (clone 1D11) was a kind gift from Merck Research Laboratories.

Purification of the Cardiac SR Ca-ATPase. Sarcoplasmic reticulum (SR) vesicles were isolated from porcine ventricles as previously described (*27*), and the Ca-ATPase was affinity purified from SR using Reactive Red-Sepharose (*28*). Protein was assayed by the Amidoschwartz method using bovine serum albumin as the standard (*29*).

PLB Purification. A fraction enriched in PLB purified from porcine cardiac SR by a procedure previously described for canine cardiac SR (*30*) was solubilized in 1.25% SDS, 1 mM $MgCl_2$, 5 μM $CaCl_2$, 0.14 M β-mercaptoethanol, 0.5% bromophenol blue, and 50% glycerol and heated at 95 °C for 2 min before application to 15% SDS−PAGE (*31*). Monomeric PLB migrating in the 6−8 kDa range, as identified by Western immunoblots, was excised for electroelution with 0.01 M Tris−acetate (pH 8.6). Finally, the electroeluted sample was dialyzed against double distilled water, concentrated in a Centriprep-3 (Amicon) ultrafiltration concentrator, and lyophilized.

Reconstitution of Cardiac SR Ca-ATPase with PLB. Affinity-purified SERCA2a was co-reconstituted with PLB, essentially as previously described in Method I by Reddy and co-workers (*32*). Briefly, the following phospholipid mixture was made in chloroform: by weight, 30% egg phosphatidylcholine, 27% egg phosphatidylethanolamine, 5% egg phosphatidic acid, 15% brain phosphatidylserine, 10% egg sphingomyelin, and 13% soybean phosphatidylinositol. This mixture was dried under nitrogen gas and redissolved in 100 mM potassium oxalate and 100 mM histidine (pH 7.0) using a bath sonicator. The resulting liposomes (0.84 mg) were mixed with 60 μg of lyophilized PLB, followed by dropwise addition of 10% 1-*O*-octyl-β-D-glucopyranoside (OG) with continual stirring until the suspension became clear. Affinity-purified cardiac Ca-ATPase (200 μg) in $C_{12}E_8$ was added to the mixed PLB−lipid−detergent micelles for a final lipid:protein ratio of approximately 3:1 (w/w) and a PLB:Ca-ATPase molar ratio of 5:1. Detergent was removed by addition of three sequential portions of 80 mg of BioBeads (Biorad SM2) per milliliter of lipid solution in 3 h, finally removing the BioBeads by filtering over glass wool. The reconstituted samples were concentrated by ultracentrifugation at 32 000 rpm ($125000g_{max}$) for 1 h in a Beckman 50.2 Ti rotor, and the resuspended pellet was applied to a stepwise sucrose gradient consisting of the following layers (w/v): 2.5%, 5%, 10%, 15%, and 20% sucrose in 100 mM K_2SO_4, 10 mM PIPES (pH 7.0). The gradient was centrifuged at $135000g_{max}$ (Beckman, SW 60Ti rotor) for 16 h at 4 °C. Fractions were collected and resuspended in 10% (w/v) sucrose, 100 mM K_2SO_4, 10 mM PIPES (pH 7.0). Based on analysis by immunoblots (using antibodies directed against either PLB or SERCA2a), fractions migrating at the 5/10% and 10/15% interfaces were pooled for use in further experiments as a homogeneous population of vesicles containing both PLB and the Ca-ATPase.

ATPase Activity. Calcium-dependent ATPase activity was measured in a solution containing 0.1 mg of protein/mL, 0.1 M KCl, 5 mM $MgCl_2$, 6 μM A23187, 25 mM MOPS (pH 7.0), 0.1 mM EGTA, and sufficient $CaCl_2$ to provide the desired free calcium concentrations. Free calcium concentrations were calculated from total calcium and EGTA concentrations taking into account pH and Mg^{2+} and nucleotide concentrations (*33*). The reaction was started by the addition

of 5 mM ATP, and the initial rate of release of inorganic phosphate was measured (*34*).

Gel Electrophoresis. Sodium dodecyl sulfate−polyacrylamide gel electrophoresis was performed by the method of Laemmli (*31*), using 7.5% (w/v) or 15% (w/v) polyacrylamide gels with a 3% stacking gel.

Western Immunoblotting. Protein from SDS−PAGE was blotted onto nitrocellulose paper as described previously (*35*). Primary antibodies against SERCA2a (clone IID8; Affinity Bioreagents, Neshanic Station, NJ) and PLB (clone 1D11; Merck, Inc.) were diluted 1:10 000 and 1:500, respectively, for incubation with the nitrocellulose paper. Binding of primary antibody was visualized by peroxidase-linked goat anti-rabbit antibody (Zymed, South San Francisco, CA) and the peroxidase substrate 4-chloro-1-naphthol.

Calcium Uptake. Calcium uptake of the reconstituted vesicles was monitored by changes in external calcium concentration using the fluorescent calcium chelator Calcium Green-5N (Molecular Probes). Intravesicular oxalate, present as a result of the reconstitution (see above), served as a calcium precipitating agent for uptake measurements. Reconstituted liposomes (50−200 μg) were diluted in a buffer containing 100 mM KCl, 5 mM $MgCl_2$, 100 mM MOPS (pH 7.0), 200 μM EGTA, and 100 nM Calcium Green-5N. Calibration was established in the same buffered solution by addition of known calcium concentrations. Calcium uptake, initiated by addition of 1 mM ATP to the sample buffer, was measured by changes in emission at 530 nm with an ISS fluorometer (model K2) in the ratio mode; a Xenon arc lamp provided excitation.

Phospholipid Assay. SR samples were ashed with 70% perchloric acid at 180 °C overnight. The inorganic phosphate concentration was determined by reaction with 0.27% ammonium molybdate and 1.1% ascorbic acid. The absorbance is monitored at 660 nm with inorganic phosphate as a standard (*36*).

Derivatization of PLB with FITC. Freshly made FITC (16.5 μM) was incubated with 20 μg/mL PLB in 0.3 M sucrose, 0.1 M KCl, 1% 1-*O*-octyl-β-D-glucopyranoside (ICN), and 10 mM Tris (pH 9.2) for 2 h at 22 °C in the dark. The reaction was stopped by a 10-fold dilution with ice-cold 0.3 M sucrose, 0.1 M KCl, 20 mM MOPS (pH 7.0), followed by dialysis against 20 mM MOPS (pH 7.0), overnight at 4 °C. This sample was concentrated (approximately 10-fold) with a Centriprep-3 ultrafiltration concentrator at 3000g_{max} for 2−3 h. The stoichiometry of bound FITC per Ca-ATPase polypeptide chain was measured in the presence of 1% SDS, 0.1 M NaOH, using the molar extinction coefficients of 80 000 M^{-1} cm^{-1} at 495 nm for FITC and 1323 M^{-1} cm^{-1} for tyrosine absorbance at 280 nm to determine protein concentration. FITC-modified PLB was dialyzed against distilled water and lyophilized for later reconstitution.

Measurements of the Extent of Phosphorylation of PLB Induced by PKA. PLB or fully labeled FITC-PLB was reconstituted into liposomes of extracted SR lipids. Subsequently, these (0.05 mg/mL) proteoliposomes were incubated at room temperature for 10 min with 60 μg/mL PKA, 1 μM cAMP, 5 mM [γ-^{32}P]ATP (4500 cpm/nmol), 100 mM KCl, 5 mM $MgCl_2$, 100 μM EGTA, 103 μM $CaCl_2$, 25 mM MOPS (pH 7.0). The calculated free calcium concentration was 0.5 μM. The reaction was stopped by filtration on a glass filter, followed by washing with nonradioactive reaction buffer. Radioactivity associated with each filter was measured by scintillation counting. Nonspecific radioactivity measured in the absence of PKA was subtracted from the total radioactivity.

Fluorescence Measurements. FITC-PLB was excited at 485 nm, and emitted fluorescence was detected after a Schott OG-530 long-pass filter using a Glan−Thompson polarizer set parallel or perpendicular to the vertically polarized excitation light. Steady-state polarization (*P*) was calculated from the ratio of the fluorescence intensities (*I*) measured with the polarizers on the excitation and emission sides of the sample in the vertical (v) or horizontal (h) position. (For example, I_{vh} refers to the fluorescence intensity measured with the excitation polarizer in the vertical position and emission polarizer in the horizontal position.) *P* is calculated from the equation:

$$P = \frac{I_{vv} - GI_{vh}}{I_{vv} + GI_{vh}} \tag{1}$$

where $G = I_{hv}/I_{hh}$ and corrects for the differing sensitivities of the detection system for vertically and horizontally polarized light (*37*).

Data Analysis. Decreases in the emission anisotropy [$A = (1/P - 1/3)^{-1}$] of FITC bound to PLB upon increasing the labeling stoichiometry result from fluorescence resonance energy transfer (FRET), and provide information regarding subunit interactions between neighboring PLB molecules (*38*−*40*), where

$$A(A_0,A_s,A_t) = \sum_{r=1}^{N} \frac{(N-1)!}{(r-1)!(N-r)!} (f)^{r-1}(1-f)^{N-r} \times \left[A_0 - (A_0 - A_s) \frac{\dfrac{(r-1)(A_0 - A_s)}{(N-1)(A_s - A_t)}}{1 + \dfrac{(r-1)(A_0 - A_s)}{(N-1)(A_s - A_t)}} \right] \tag{2}$$

$A(A_0,A_s,A_t)$ is the measured emission anisotropy, *f* is the labeling stoichiometry of FITC per mole of PLB, *N* is the apparent oligomeric size of PLB, A_0 is the initial emission anisotropy in the absence of FRET, A_s is the emission anistropy when all FITC labeling sites within the Ca-ATPase oligomeric complex are saturated, and A_t is the emission anisotropy after one FRET event. Fitting the data involves incrementally adjusting *N* by integral values and solving for A_0, A_s, and A_t, which provide information regarding both the spatial separation and orientation of chromophores on adjacent Ca-ATPase polypeptide chains (*38*). Knowledge of A_0, A_s, A_f, and the Förster distance (R_0) permits calculation of the average separation (*r*) between FITC chromophores, where

$$r = R_0 \left[\frac{(2A_t/A_0) + 1}{3} \right]^2 \frac{(A_s - A_t)}{(A_0 - A_s)(N-1)} \tag{3}$$

In the presence of a heterogeneous population of PLB molecules with two known oligomeric states, N_a and N_b, the

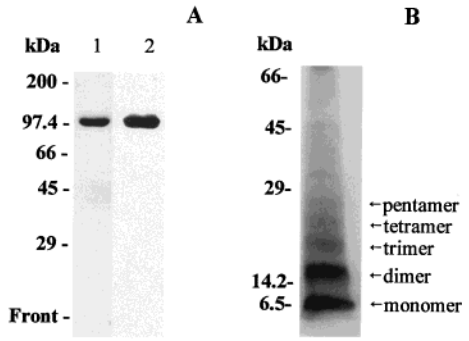

FIGURE 1: Protein composition of reconstituted proteoliposomes. 9% Laemmli gels (panel A) of reconstituted proteoliposomes stained with Coomassie blue (lane 1) and after immunoblotting and detection using primary antibody directed against the Ca-ATPase (lane 2). Panel B represents an immunoblot using anti-PLB antibody after separation with a 13% resolving gel of the same reconstituted proteoliposomes. The relative migrations of molecular mass markers are indicated on the left side of each panel; markers include myosin (200 kDa), phosphorylase *b* (97.4 kDa), bovine serum albumin (66 kDa), ovalbumin (45 kDa), soybean trypsin inhibitor (29 kDa), lysozyme (14.2 kDa), and aprotinin (6.5 kDa).

fractional contribution of each species can be determined from

$$A_{\text{observed}} = [f_a A_a(N_a)] + [(1 - f_a)A_b(N_b)] \qquad (4)$$

In fitting the emission anisotropy as a function of the fractional saturation of fluorophore sites, various integral values of N were specified, and for each value, a three-parameter fit was performed with optimal values of A_0, A_t, and A_s. Minimal chi-squared values of the fits indicated which value of N best described the data.

RESULTS

Functional Characterization of Reconstituted Proteoliposomes. Phospholamban (PLB) and the Ca-ATPase were separately purified from porcine cardiac SR (*28, 30*). Subsequently, these purified proteins were co-reconstituted at a molar ratio of five PLB to one Ca-ATPase into vesicles of mixed phospholipids (*32, 41*). A homogeneous population of reconstituted proteoliposomes containing both the Ca-ATPase and PLB with a buoyant density between 5% (w/v) and 15% (w/v) sucrose was obtained using a sucrose density gradient; this vesicle fraction was shown to be enriched in both PLB and the Ca-ATPase based on gels and immunoblots with antibodies directed against these respective proteins (Figure 1). These proteoliposomes have a lipid content similar to that of native cardiac SR membranes (0.8 mg/mg), and are tightly sealed and fully functional as evidenced by high rates of calcium-dependent ATPase activity that are stimulated upon addition of the calcium ionophore A23187 to a similar extent as that observed using native cardiac SR vesicles. Alternatively, the Ca-ATPase was reconstituted with PLB that was expressed and purified from *E. coli* (*42*). The calcium dependences of the catalytic activity for the Ca-ATPase in these reconstituted vesicles are virtually identical to those observed using native cardiac SR membranes, and the extent of activation of these membranes by saturating concentrations of calcium or following addition of cAMP-dependent protein kinase (PKA) at submicromolar calcium concentrations is comparable to that observed for native cardiac SR (Figure 2). Thus, these reconstituted proteoliposomes contain substantial populations of both Ca-ATPase and PLB that are asymmetrically oriented and conformationally competent to allow the functional interactions and the structural transitions required for increased calcium transport in response to the phosphorylation of PLB.

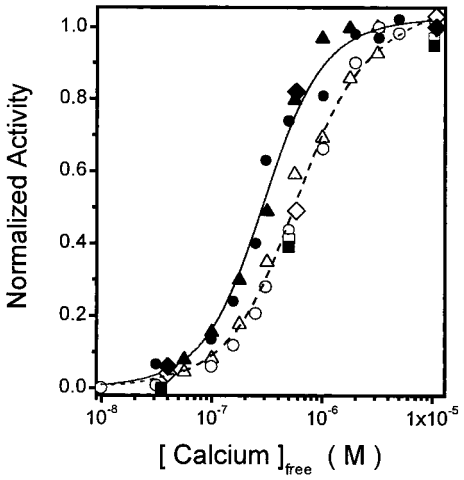

FIGURE 2: Functional regulation of reconstituted Ca-ATPase by PLB. Calcium concentration dependence of normalized calcium-dependent ATPase activity of native porcine cardiac SR (○,●) compared with activities for the cardiac Ca-ATPase co-reconstituted with either PLB (◇,◆) or FITC-PLB (□,■) isolated from cardiac SR or using recombinant PLB expressed and purified from *E. coli* (△,▲) in the absence (○,◇,□,△) or presence (●,◆,■,▲) of 1 μM cAMP and 80 μg/mL bovine heart PKA. Initial rates of ATP hydrolysis were measured at 25 °C in a medium of 0.1 mg of protein/mL containing 25 mM MOPS (pH 7.0), 0.1 M KCl, 5 mM ATP, 6 μM A23187, 5 mM $MgCl_2$, 0.1 mM EGTA, and sufficient $CaCl_2$ for the free calcium concentrations indicated. All specific activities were normalized relative to the maximal activity of each sample. Maximal calcium-dependent ATPase activities were 2.2 and 1.1 μmol min^{-1} mg^{-1} for reconstituted and cardiac SR samples, respectively. Maximal calcium uptake activities for reconstituted samples and cardiac SR were 4 ± 1 μmol min^{-1} mg^{-1} and 1.9 ± 0.1 nmol min^{-1} mg^{-1}, respectively. Symbols represent the means of four determinations using two separate preparations. Standard errors were less than 5% of the indicated values.

Oligomeric Interactions between PLB in Reconstituted Proteoliposomes. To determine the average oligomeric size of PLB in these reconstituted membranes, we have used fluorescence resonance energy transfer (FRET) measurements, taking advantage of the ability to selectively and covalently modify the single primary amine in PLB (Lys^3) with fluorescein isothiocyanate (FITC) prior to its co-reconstitution with the Ca-ATPase (*44*). The resulting preparation exhibits an equivalent calcium dependence to that of native cardiac SR prior to PLB phosphorylation, indicating that FITC does not affect the ability of PLB to inhibit Ca-ATPase activity. Fluorescein with its large quantum yield and small Stokes shift results in substantial spectral overlap between the emission and absorption spectra that allows this fluorophore to serve as both an energy transfer donor and acceptor (*39*). Thus, two molecules of FITC within a critical distance of one another can transfer nonradiative energy (homotransfer) as in the case of different donor and acceptor probes (heterotransfer). With a Förster critical distance (R_0) of 50 Å, homotransfer between fluorescein chromophores has been shown to provide a sensitive measure of oligomeric protein associations (*38*−*40, 45*). Based on the strong depolarization of fluorescence emission by homotransfer, we

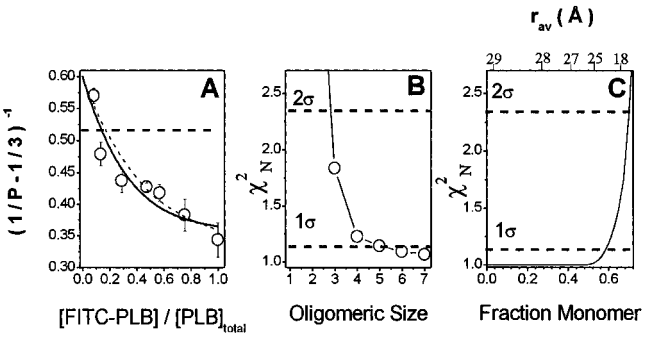

FIGURE 3: Oligomeric interactions between PLB molecules. Panel A shows FITC anisotropy data as a function of the fraction of FITC-PLB, where data points represent the average values obtained from four independent measurements and the error bars are the standard errors of the mean. Solid and dotted lines, respectively, represent least-squares fits of the data to eq 2 under Experimental Procedures corresponding to a pentamer or monomer, assuming a single oligomeric state for PLB. The dashed line indicates the best fit assuming a distribution of oligomeric states for PLB obtained from a densitometric analysis of immunoblots (see lane 3, Figure 2), corresponding to 47% monomer and 53% pentamer. Panel B shows the normalized chi-squared values (χ^2_N) for fits assuming that PLB is a homogeneous population of different oligomeric sizes, where the *F*-statistics corresponding to one and two standard deviations (σ) from the optimal fit are shown as horizontal dotted lines. Panel C shows the normalized χ^2_N values determined from a least-squares fit to the data, using a two-state model, where varying fractions of monomeric PLB are assumed with the remainder of the PLB assumed to be pentameric (see eq 4 under Experimental Procedures). Corresponding values for the average distance (r_{av}) between FITC chromophores on adjacent PLB molecules for a pentameric association are shown on the top axis, as determined using eq 3 under Experimental Procedures.

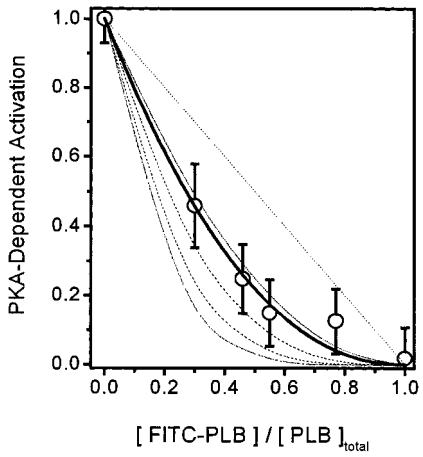

FIGURE 4: Relationship between activation of Ca-ATPase activity by PKA and fraction of FITC-PLB. Calcium-dependent ATPase activity of the cardiac Ca-ATPase co-reconstituted with different ratios of fully FITC-derivatized and unlabeled PLB was measured as described under Experimental Procedures. Data are plotted as activity in the presence minus that in the absence of cAMP and PKA as a function of moles of FITC per mole of ATPase. Data points represent the average values of four independent measurements using two different preparations, where error bars represent the standard errors of the mean. Lines represent models for first- through fifth-order inactivation, i.e., where activation = (FITC stoichiometry)^n, where *n* is varied between 1 and 5. Experimental conditions are as described in the legend to Figure 1, except that the free calcium concentration was maintained at 0.5 μM.

have used measurements of fluorescence polarization (anisotropy) to determine the average oligomeric size of PLB. The presence of multiple energy transfer neighbors results in greater depolarization of fluorescence emission and thus the measured anisotropy is dependent upon the number of energy transferring units within a cluster of neighbors.

Steady-state anisotropy, plotted in the form of a Perrin equation, i.e., $(1/P - 1/3)^{-1}$, was measured for samples co-reconstituted with varying fractions of unlabeled and FITC-labeled PLB relative to the Ca-ATPase (Figure 3A). Upon increasing the fractional incorporation of FITC-PLB, a progressive decrease in the measured anisotropy is observed, implying the mixing of labeled and unlabeled populations of PLB in reconstituted proteoliposomes and concomitant increases in energy transfer between FITC molecules as the amount of available probe sites are saturated. The anisotropy value at the lowest labeling stoichiometry, which is near the theoretical maximum (rigid limit) of 0.6, demonstrates a highly ordered environment around FITC, consistent with earlier suggestions that the amino terminus of PLB exhibits considerable structure (*12*, *14*). The decrease in the emission anisotropy upon increasing the fraction of FITC-PLB indicates the presence of subunit interactions between PLB molecules, as illustrated by the contrast between a model for monomers, represented by the dashed horizontal line in Figure 3A, and the data (see eq 2 under Experimental Procedures). The data were further fit to a series of models in which the oligomeric state (*N*) was set at various integer values ranging from 1 to 10. The relative goodness of fit, as assessed by the reduced chi-squared values (χ_R^2), suggests that the data are best described (based on chi-squared values less than 1 σ) by a model in which the average oligomeric state (*N*) of PLB is a pentamer or larger (Figure 3B), in agreement with earlier results (*18*, *19*). From these fits, the mean distances recovered between FITC fluorophores on neighboring PLB molecules vary between 28 and 31 Å upon increasing the value of *N* from 5 to 10. These distances are less than $0.8R_0$, which has been shown to be optimal for resolving the number of subunits in an oligomer by measurements of homotransfer (*40*).

While these anisotropy data are consistent with large oligomers as the predominant cluster group in these membranes, the data can be equally well fit to a model that assumes two populations of oligomers (Figure 3A, dotted line). Thus, assuming that PLB exists predominantly as a mixture of monomers and pentamers, it is possible to estimate the relative amounts of each species based on the goodness of fit of the data to various models. An upper limit for the concentration of monomeric species is estimated at ~59% of the total PLB (Figure 3C). These data are consistent with suggested models having two populations of PLB species: one, pentameric self-associating PLBs; and a second, monomeric species that interact with the Ca-ATPase (*18*, *19*, *23*).

Functional Interactions between PLB Molecules. To identify the oligomeric species of PLB relevant to their function as an inhibitor of the Ca-ATPase, we have taken advantage of the ability of FITC to inhibit PLB activation without interfering with its normal inhibitory interactions of the Ca-ATPase. For example, concomitant with the reconstitution of increasing fractions of FITC-PLB, we observe a decrease in the ability of PKA to activate the Ca-ATPase; complete loss of activation coincides with full derivatization of PLB (Figure 4). At the same time, fully labeled PLB exhibits normal inhibition of the Ca-ATPase as evidenced by Ca-ATPase activities measured at diagnostic calcium

Table 1: PKA-Dependent Phosphorylation of Reconstituted FITC-Labeled PLB

sample[a]	phosphorylated PLB[b] (nmol of ^{32}P/mol of PLB)
Ca-ATPase−PLB	0.3 ± 0.1
Ca-ATPase−FITC−PLB	0.4 ± 0.1

[a] PLB- or FITC-labeled PLBs were separately reconstituted with the Ca-ATPase into liposomes of extracted SR lipids as described under Experimental Procedures. [b] The extent of phosphorylation by PKA was assessed by incubation of 0.05 mg/mL reconstituted proteoliposomes with 60 μg/mL PKA, 1 μM cAMP, 5 mM [^{32}P]ATP, 0.1 M KCl, 5.0 mM $MgCl_2$, 100 μM EGTA, 103 μM $CaCl_2$, 25 mM MOPS (pH 7.0) for 10 min at room temperature. The incubation mixture was subsequently filtered and washed, and bound radioactivity was counted by scintillation counting. Nonspecific radioactivity, measured by incubation of proteoliposomes in the absence of PKA before filtration, washing, and counting, was subtracted from the total radioactivity. Under these conditions, 44 ± 9% of the cytosolic portions of PLB (covalently modified with dansyl chloride) was released into the supernatant.

concentrations that fall on the calcium activation curve of unlabeled PLB (Figure 2). The reduced ability of PKA to reverse the inhibition of FITC-PLB of the Ca-ATPase suggests that the fluorescein moiety of FITC may either prevent phosphorylation of Ser^{16} in PLB by PKA or, alternatively, prevent phosphorylation-dependent structural transitions responsible for activation of the Ca-ATPase. Direct measurements of the extent of phosphorylation of PLB after exposure to [^{32}P]ATP under PKA phosphorylating conditions demonstrate that FITC modification does not alter the ability of PLB to be phosphorylated (Table 1). However, irrespective of the mechanism, the loss of PKA activation induced by modification of PLB with FITC allows the titration of the fraction of activatable PLB molecules following co-reconstitution of the Ca-ATPase. As a consequence, information regarding functional interactions between PLB molecules is available from a consideration of the relationship between the decrease in the PKA-dependent activation of the Ca-ATPase and the fraction of FITC-PLB, where the

$$\text{extent of PKA-dependent activation} = \left[1 - \frac{[\text{FITC-PLB}]}{[\text{FITC-PLB}] + [\text{PLB}]}\right]^n$$

The resulting inactivation data reveal that there is not a one-to-one loss of activation as a function of FITC modification of PLB (Figure 4). Rather the data in Figure 4 are best described by a second-order loss of activation (i.e., $n = 2.2 \pm 0.2$), suggesting the involvement of two PLB molecules with each functional unit of the Ca-ATPase.

DISCUSSION

Summary of Results. Using PLB covalently modified at Lys^3 with FITC, we have investigated both the structural arrangement and the functional interactions of PLB molecules co-reconstituted with the Ca-ATPase in lipid membranes where PLB is in molar excess of the Ca-ATPase. We have identified the average oligomeric state of PLB to be a pentamer or larger. The average spatial separation between FITC chromophores is between 21 and 31 Å, depending on the model used to analyze the data (Figure 3). These distances are consistent with earlier models regarding the structural arrangement of PLB oligomers (*14, 19*). FITC modification does not interfere with inhibitory interactions between PLB and the Ca-ATPase (Figure 1), indicating that normal structural interactions between PLB and the Ca-ATPase are maintained. However, FITC modification specifically blocks the normal activation of the Ca-ATPase by PKA, permitting a determination of the oligomeric species that regulate Ca-ATPase function. We find that upon increasing the fraction of FITC-PLB in reconstituted membranes, there is a second-order loss in the ability for PKA to activate the Ca-ATPase (Figure 4), indicating that activation of the Ca-ATPase requires the activation of multiple PLB molecules within a quaternary complex containing the Ca-ATPase. These results suggest that functional linkages between PLB polypeptide chains are important to Ca-ATPase activation, either by direct linkage or through interacting Ca-ATPase molecules (Figure 5).

Relationship to Previous Results. PLB represents a major target of the β-adrenergic cascade in the heart, and has been shown to function as a major regulator of the Ca-ATPase in cardiac SR membranes (*1, 46−48*). The enhanced calcium sensitivity of the Ca-ATPase concomitant with PLB phosphorylation results in increased myocardial contractility. The nature of the structural interaction between PLB and the Ca-ATPase has attracted considerable attention, as the disruption of this interaction may represent an important target for drug development that could enhance the calcium handling properties of the failing heart (*49*). An important aspect of this interaction is the stoichiometry between PLB and the Ca-ATPase, especially in view of the striking propensity of PLB for self-association. Self-association in SDS has been extensively documented using SDS−PAGE, which indicates that PLB migrates preferentially as monomeric and homopentameric complexes (*25, 50−52*). Consistent with the observed distribution of PLB oligomeric species in detergent, spin-label EPR spectroscopy and fluorescence resonance energy transfer measurements of PLB reconstituted within membranes demonstrate that the average oligomeric size of PLB oligomers is also a homopentamer (*18, 19*). Possible structures of the homopentamer have been suggested from a consideration of both (i) the chemical reactivity of the cysteines within the transmembrane portion of PLB to chemical modification and (ii) correlations between site-directed mutations within PLB that modify the distribution of oligomeric species on SDS−PAGE (*14, 53, 54*). These structural models are consistent with measured distances between chromophores bound to Lys^3 within neighboring PLB molecules co-reconstituted with the Ca-ATPase, which were determined to be approximately 21 Å (*19*). However, the function of oligomeric forms of PLB has been unclear, as the presence of the Ca-ATPase results in the stabilization of monomeric forms of PLB (*19*). Moreover, PLB mutants that stabilize the monomeric form of PLB are capable of full inhibition of the Ca-ATPase, suggesting that pentamers are not the activating species of PLB (*5, 19, 20, 21, 23, 55*). In contrast, full activation of the Ca-ATPase has been shown to require the phosphorylation of multiple PLB molecules by PLB (*24, 25*). These latter results are in agreement with the second-order loss of the PKA-dependent activation of the Ca-ATPase reconstituted with varying fractions of FITC-PLB (Figure 4), where FITC-PLB stabilizes the inhibitory interaction between PLB

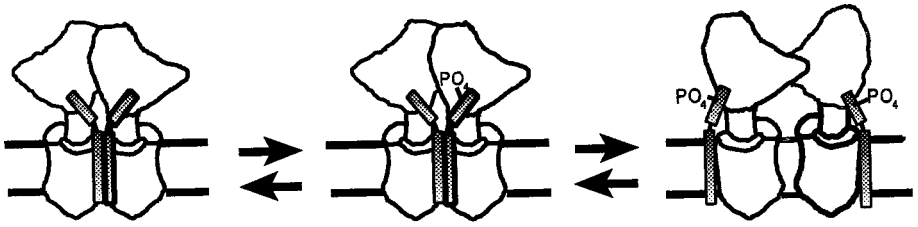

FIGURE 5: Model depicting possible interactions between PLB and the Ca-ATPase. PLB is shown as a monomeric unit interacting with each Ca-ATPase; two Ca-ATPase−PLB heterodimers interact as a functional unit. Activation of the Ca-ATPase by PKA is suggested to require the phosphorylation of two PLBs within a dimeric complex containing two Ca-ATPase polypeptide chains. Phosphorylation of PLBs results in conformational changes to both PLB and the Ca-ATPase, including the spatial rearrangement of Ca-ATPase polypeptide chains with respect to one another, as previously shown to be associated with enzyme activation by PKA (*27, 59*). Conformational changes of PLB, largely undefined as yet, exclude its dissociation from the Ca-ATPase (*61, 64, 67*). Larger oligomers of PLB (not shown) are not directly involved in the functional regulation of the Ca-ATPase. The overall shape of the Ca-ATPase is highly asymmetrical, and was derived from the 14 Å resolution image obtained using image-enhanced cryo-electron microscopy (*65*).

and the Ca-ATPase. These results suggest that activation of the Ca-ATPase requires the PKA-dependent activation of two PLB molecules, implying that endogenous phosphatases can function to ensure the Ca-ATPase remains in the less active state prior to a large increase in the activity of PKA following β-adrenergic stimulation. These results suggest that observed differences in the abilities of PLB to regulate the Ca-ATPase under in vitro and in vivo conditions may involve differences in the steady-state levels of PLB phosphorylation (*55*).

Model Illustrating Proposed Interactions between PLB and the Ca-ATPase. The second-order decrease in the extent of activation of the Ca-ATPase co-reconstituted in the presence of variable fractions of FITC-PLB observed in this study indicates a requirement for two PLB molecules in the PKA-induced activation of the Ca-ATPase (Figure 4). As an illustration of the interpretation of this kind of data, the effects on activation by random modification with FITC of 50% of the PLB molecules can be considered. For example, random modification of 50% of PLB in a dimeric arrangement with a functional unit (either monomer or oligomer) of the Ca-ATPase would result in 75% loss of PKA-induced activation of the Ca-ATPase, i.e., second-order inactivation, as observed here (Figure 5). In contrast, random modification of 50% of PLBs that are arranged as one PLB per functional unit of the Ca-ATPase would result in 50% loss of activation, i.e., first-order inactivation. For an alternate arrangement in which pentameric PLBs are associated with the Ca-ATPase in such a manner that two PLB subunits directly interact with the Ca-ATPase, random modification of 50% of the PLBs would be expected to result in a 40% loss of activation. Thus, the latter two models do not fit the inactivation data (Figure 4). While these data do not address the functional unit of the Ca-ATPase, previous cross-linking and radiation inactivation experiments have indicated a dimeric Ca-ATPase (*56*−*59*). Therefore, a possible model for these interactions involves a functional complex consisting of two heterodimers of PLB associated with the Ca-ATPase (Figure 5). The free pool of PLB may exist predominantly as oligomers that under some conditions are capable of exchange with PLB bound to the Ca-ATPase (*19, 22*). That the monomeric form of PLB is able to fully regulate Ca-ATPase function suggests a monomeric intermediate between free oligomers and bound PLB peptides (*19, 20, 23*).

This model also reflects previous experimental observations. Based on site-directed mutagenesis, sequences in both transmembrane and cytosolic portions of PLB and the Ca-ATPase are critical to the inhibition of Ca-ATPase function, and are presumably involved in intraprotein interactions (*4, 5, 20, 60, 66*). FRET between fluorophores on Ca-ATPase polypeptide chains and rotational diffusion measurements demonstrate that PLB phosphorylation results in the reorientation of Ca-ATPase polypeptide chains with respect to one another within defined oligomers (*27, 59, 61*). PLB phosphorylation alters the interaction between PLB and the Ca-ATPase, without dissociation of the cytosolic domain of PLB from the Ca-ATPase (*62, 63, 64*).

CONCLUSIONS

We have demonstrated that PLB self-associates to form large oligomers consisting of five or more subunits following functional reconstitution with the Ca-ATPase, but that the oligomeric state of PLB in association with the Ca-ATPase is considerably smaller. Thus, while FITC-PLB undergoes normal inhibitory interactions with the Ca-ATPase, the second-order loss in the ability to activate the Ca-ATPase by PKA upon reconstitution of varying fractions of FITC-PLB indicates that the activation of multiple PLB molecules is necessary for activation of the Ca-ATPase. Since site-directed mutations that stabilize the monomer of PLB are able to fully activate the Ca-ATPase, these results suggest that a single PLB molecule binds to each Ca-ATPase to form a functional complex consisting of two heterodimers (Figure 5). Thus, in the presence of saturating PLB (as used in this study), PKA-dependent activation of both molecules of PLB is necessary to promote conformational changes within individual Ca-ATPase polypeptide chains necessary for enzyme activation. This mechanism of regulation has the potential to fine-tune the activation of the Ca-ATPase through the β-adrenergic cascade, such that a threshold level of PKA activation is necessary to result in enhanced Ca-ATPase activity.

REFERENCES

1. Kirchberger, M. A., Tada, M., and Katz, A. M. (1974) *J. Biol. Chem. 249*, 6166−6173.
2. Simmerman, H. K. B., and Jones, L. R. (1998) *Physiol. Rev. 78*, 921−947.
3. Koss, K. L., and Kranias, E. G. (1996) *Circ. Res. 79*, 1059−1063.
4. Toyofuku, T., Kurzydlowski, K., Tada, M., and MacLennan, D. H. (1993) *J. Biol. Chem. 268*, 2809−2815.
5. Toyofuku, T., Kurzydlowski, K., Tada, M., and MacLennan, D. H. (1994) *J. Biol. Chem. 269*, 3088−3094.
6. Kimura, Y., Kurzydlowski, K., Tada, M., and MacLennan, D. H. (1996) *J. Biol. Chem. 271*, 21726−21731.

7. Simmerman, H. K. B., Lovelace, D. E., and Jones, L. R. (1989) *Biochim. Biophys. Acta 997*, 322−329.
8. Terzi, E., Poteur, L., and Trifilieff, E. (1992) *FEBS Lett. 309*, 413−416.
9. Vorherr, T., Chiesi, M., Schwaller, R., and Carafoli, E. (1992) *Biochemistry 31*, 339−347.
10. Mortishire-Smith, R. J., Pitzenberger, S. M., Burke, C. J., Middaugh, C. R., Garsky, V. M., and Johnson, R. G. (1995) *Biochemistry 34*, 7603−7613.
11. Tatulian, S. A., Jones, L. R., Reddy, L. G., Stokes, D. L., and Tamm, L. K. (1995) *Biochemistry 34*, 4448−4456.
12. Li, M., Cornea, R. L., Autry, J. M., Jones, L. R., and Thomas, D. D. (1998) *Biochemistry 37*, 7869−7877.
13. Fujii, J., Ueno, A., Kitano, K., Tanaka, S., Kadoma, M., and Tada, M. (1987) *J. Clin. Invest. 79*, 301−304.
14. Arkin, I. T., Rothman, M., Ludlam, C. F., Aimoto, S., Engelman, D. M., Rothschild, K. J., and Smith, S. O. (1995) *J. Mol. Biol. 248*, 824−834.
15. Mortishire-Smith, R. I., Broughton, H., Garsky, V. M., Mayer, E. J., and Johnson, R. G. (1998) *Ann. N.Y. Acad. Sci. 853*, 63−78.
16. Wegener, A. D., Simmerman, H. K., Liepnieks, J., and Jones, L. R. (1986) *J. Biol. Chem. 261*, 5154−5159.
17. Mayer, E. J., McKenna, E., Garsky, V. M., Burke, C. J., Mach, H., Middaugh, C. R., Sardana, M., Smith, J. S., and Johnson, R. G., Jr. (1996) *J. Biol. Chem. 271*, 1669−1677.
18. Cornea, R. L., Jones, L. R., Autry, J. M., and Thomas, D. D. (1997) *Biochemistry 36*, 2960−2967.
19. Reddy, L. G., Jones, L. R., and Thomas, D. D. (1999) *Biochemistry 38*, 3954−3962.
20. Kimura, Y., Kurzydlowski, K., Tada, M., and MacLennan, D. H. (1997) *J. Biol. Chem. 272*, 15061−15064.
21. Autry, J. M., and Jones, L. R. (1997) *J. Biol. Chem. 272*, 15872−15880.
22. Thomas, D. D., Reddy, L. G., Karim, C. B., Cornea, R., Autry, J. M., Jones, L. R., and Stamm, J. (1998) *Ann. N.Y. Acad. Sci. 853*, 186−194.
23. Reddy, L. G., Autry, J. M., Jones, L. R., and Thomas, D. D. (1999) *J. Biol. Chem. 274*, 7649−7655.
24. Kranias, E. G. (1985) *J. Biol. Chem. 260*, 11006−11010.
25. Coyler, J., and Wang, J. H. (1991) *J. Biol. Chem. 266*, 17486−17493.
26. Young, E. F., McKee, M. J., Ferguson, D. G., and Kranias, E. G. (1989) *Membr. Biochem. 8*, 95−106.
27. Negash, S., Chen, L. T., Bigelow, D. J., and Squier, T. C. (1996) *Biochemistry 35*, 11247−11259.
28. Yao, Q., Chen, L. T., and Bigelow, D. J. (1998) *Protein Expression Purif. 13*, 191−197.
29. Schaffner, W., and Weissmann, C. (1973) *Anal. Biochem. 56*, 502−514.
30. Jones, L. R., Simmerman, H. K. B., Wilson, W. W., Guard, F. R. N., and Wegener, A. D. (1985) *J. Biol. Chem. 260*, 7721−7730.
31. Laemmli, U. K. (1970) *Nature 227*, 680−685.
32. Reddy, L. G., Jones, L. R., Cala, S. E., O'Brian, J. J., Tatulian, S. A., and Stokes, D. L. (1995) *J. Biol. Chem. 270*, 9390−9397.
33. Fabiato, A. (1988) *Methods Enzymol. 157*, 378−417.
34. Lanzetta, P. A., Alvazez, L. J., Reinsch, P. S., and Candia, D. A. (1979) *Anal. Biochem. 100*, 95−97.
35. Renart, J., and Sandoval, I. V. (1984) *Methods Enzymol. 104*, 455−460.
36. Chen, P. S., Toribara, T. Y., and Warner, H. (1956) *Anal. Chem. 28*, 1756−1758.
37. Lakowicz, J. R. (1983) *Principles of Fluorescence Spectroscopy*, Plenum Press, New York.
38. Weber, G., and Daniel, E. (1966) *Biochemistry 5*, 1900−1907.
39. Highsmith, S., and Cohen, J. A. (1987) *Biochemistry 26*, 154−161.
40. Runnels, L. W., and Scarlata, S. F. (1995) *Biophys. J. 69*, 1569−1583.
41. Levy, D., Gulik, A., Bluzat, A., and Rigaud, J.-L. (1992) *Biochim. Biophys, Acta 1107*, 283−298.
42. Yao, Q., Bevan, J. L., Weaver, R. F., and Bigelow, D. J. (1996) *Protein Expression Purif. 8*, 463−468.
43. Ferrington, D. A., Moewe, P. L., Yao, Q., and Bigelow, D. J. (1998) *Biophys. J. 74*, 356a.
44. Haugland, R. (1996) *Handbook of Fluorescent Probes and Research Chemicals*, Molecular Probes, Inc., Eugene, OR.
45. Erijman, L., and Weber, G. (1991) *Biochemistry 30*, 1595−1599.
46. Kranias, E. G., and Solaro, R. J. (1982) *Nature 298*, 182−184.
47. Luo, W., Grupp, I. L., Harrer, J., Ponniah, S., Grupp, G., Duffy, J. J., Doetschman, T., and Kranias, E. G. (1994) *Circ. Res. 75*, 401−409.
48. Wolska, B. M., Stojanovic, M. O., Luo, W., Kranias, E. G., and Solaro, R. J. (1996) *Am. J. Physiol. 271*, C391−C397.
49. Johnson, R. G., Jr. (1998) *Ann. N.Y. Acad. Sci. 853*, 380−392.
50. Wegener, A. D., and Jones, L. R. (1984) *J. Biol. Chem. 259*, 1834−1841.
51. Tada, M., Kadoma, M., Inui, M., and Fujii, J. (1988) *Methods Enzymol. 157*, 107−154.
52. Li, C., Wang, J. H., and Coyler, J. (1990) *Biochemistry 29*, 4535−4540.
53. Arkin, I. T., Adams, P. D., Brünger, A. T., Smith, S. O., and Engelman, D. M. (1997) *Annu. Rev. Biophys. Biomol. Struct. 26*, 157−179.
54. Karim, C. B., Stamm, J. D., Karim, J., Jones, L. R., and Thomas, D. D. (1998) *Biochemistry 37*, 12074−12081.
55. Chu, G., Li, L., Sato, Y., Harrer, J. M., Kadambi, V. J., Hoit, B. D., Bers, D. M., and Kranias, E. G. (1998) *J. Biol. Chem. 273*, 33674−33680.
56. Chamberlain, B. K., Berenski, C. J., Jung, C. Y., and Fleischer, S. (1983) *J. Biol. Chem. 258*, 11997−12001.
57. Hymel, L., Maurer, A., Berenski, C., Jung, C. Y., and Fleischer, S. (1984) *J. Biol. Chem. 259*, 4890−4895.
58. Squier, T. C., Hughes, S. E., and Thomas, D. D. (1988) *J. Biol. Chem. 263*, 9162−9170.
59. Chen, L., Yao, Q., Brungardt, K., Squier, T. C., and Bigelow, D. J. (1998) *Ann. N.Y. Acad. Sci. 853*, 264−266.
60. MacLennan, D. H., Kimura, Y., and Toyofuku, T. (1998) *Ann. N.Y. Acad. Sci. 853*, 31−42.
61. Negash, S., Sun, H., Yao, Q., Goh, S., Bigelow, D., and Squier, T. (1998) *Ann. N.Y. Acad. Sci. 853*, 288−291.
62. James, P., Inui, M., Tada, M., Chiesi, M., and Carafoli, E. (1989) *Nature 342*, 90−92.
63. Negash, S., Huang, S., and Squier, T. C. (1999) *Biochemistry 38*, 8150−8158.
64. Levine, B. A., Patchell, V. B., Sharma, P., Gao, Y., Bigelow, D. J., Yao, Q., Goh, S., Colyer, J., Drago, G. A., and Perry, S. V. (1999) *Eur. J. Biochem. 264*, 905−913.
65. Toyoshima, C., Sasabe, H., and Stokes, D. L. (1993) *Nature 362*, 469−471.
66. Asahi, M., Kimura, Y., Kurzydlowski, K., Tada, M., and MacLennan, D. H. (1999) *J. Biol. Chem. 274*, 32855−32862.
67. Negash, S., Yao, Q., Sun, H., Li, J., Bigelow, D. J., and Squier, T. C. (2000) *Biochem. J. 351*, 195−205.

BI002891T